Factor Analysis of Scintigraphic Image Sequences with Integrated Probabilistic Mask of Factor Images

Ondřej Tichý*

2nd year of PGS, email: otichy@utia.cas.cz
Department of Mathematics
Faculty of Nuclear Sciences and Physical Engineering, CTU in Prague

advisor: Václav Šmídl, Institute of Information Theory and Automation, Department of Adaptive Systems, AS CR

Abstract. Factor analysis is a well established mathematical method for factor separation in the analysis of scintigraphical sequences. The results are typically an input to the next step, e.g. factor analysis for computing significant diagnostic coefficients. However, this computing highly depends on proper identification of factors and their biological meaning, which is not ensure only by factor analysis. The main issue is separation overlaping factors from themselves and from tissue background covering the whole sequence. Factor analysis highly depends on prior information which allows us to set biologically reasonable conditions to a mathematical model. In this paper, we propose a mathematical model which estimates the probability mask of each image factor and sets it as a prior information for the next step of iterative algorithm based on Variational Bayes method. The new proposed model provides more realistic estimates of factors than the standard factor analysis.

Keywords: Nuclear Medicine, Scintigraphy, Factor Analysis, Factor Separation

Abstrakt. Jednou ze známých matematických metod pro analýzu scintigrafických obrazových sekvencí je faktorová analýza. Cílem diagnostiky je určit důležité diagnostické koeficienty, k tomu je ovšem potřeba detekovat jednotlivé, biologicky smysluplné, faktory, což nelze zajistit samotnou faktorovou analýzou. Základním problémem při analýze sekvence je překryv jednotlivých orgánů a jejich částí a odseparování krevního a tkáňového pozadí, které se vyskytují v celé sekvenci, přičemž faktorová analýza umožňuje zabudovat biologické předpoklady vedoucí ke smysluplnému řešení problému. V tomto příspěvku je představen nový matematický model, který odhaduje pravděpodobnost příslušnosti jednotlivých pixelů k faktorovým obrázkům a tuto informaci využívá k nastavení apriorna pro další krok výpočtu založeném na metodě Variační Bayes. Tento model dává realističtější odhady faktorů než standardní faktorová analýza.

Klíčová slova: Nukleární Medicína, Scintigrafie, Faktorová Analýza, Separace Faktorů

1 Introduction

Scintigraphy is a well known and very important method in nuclear medicine. Diagnosis using scintigraphy includes following steps. At first, a tagged radiopharmaceutical is applied into a human body lying under the scintillation camera. At second, in every

*Institute of Information Theory and Automation, Department of Adaptive Systems, AS CR

10 seconds an image of distribution of radiopharmaceutical is saved; consequently, the functional image sequence with the scanned region of interest is obtained. Further analysis of measurement is necessary for propper diagnosis. In this paper, we are focused on renal scintigraphy.

A kidney is composed of parenchyma and pelvis. In biological constraint, in about the first 120 - 180 seconds fills only parenchyma of kidney [2]; then the radiopharmaceutical passes from parenchyma to pelvis and next to the urinary bladder. This is very important information for biologically meaningful solution and verification of a mathematical model, see Section 4.1. Another assumption, the shape of convolution kernel of factor curve, will be studied in Section 4.2. For further analysis, factor identification is necessary. This is typically done by expert manually or by factor analysis automatically [1]. Finally, the resulting factors can be analyzed to set the proper diagnosis. This analysis can be done by expert or by semi-automatic algorithm based on more or less sophisticated mathematical background: Patlak-Rutland plot [4], or post-processing by deconvolution [6]. The result highly depends on the first step, correct separation, identification, and detection of factors.

Factor analysis is a statistical method based on data decomposition to the factors. Its usage is mostly scintigraphy [1], ultrasound [7], or PET [5]. However, the solution of factor analysis is ambiguous and allows infinitely many solutions. Some restrictions have been made for biologically meaningful solution, e.g. positivity of factors [10]; nevertheless, the uniqueness of solution or even biologically meaningful solution is not guaranteed only by positivity. Uniqueness can be guaranteed when each factor has at least one pixel where the others have no activity [11], but this assumption does not hold in scintigraphy because of residue activity in the whole sequence. Additional constraints are necessary to restrict the space of possible solutions.

The analytical solution of the presented model is intractable; therefore, an additional approximations have been made. The Variational Bayes approximation methodology [8] was successfully used in fields related to factor decomposition, e.g. principal component analysis, factor analysis, or models with convolution. In addition, Variational Bayes approximation offers reasonable ratio between options of modeling and computation difficulties.

2 Variational Factor Analysis (FA)

We briefly review Variational Factor Analysis. The sequence obtained by scintillation camera contains n images taken at time $t = 1 \dots n$, typically after 10 seconds. Every image is a compound of p pixels; consequently, the images are saved in p-dimensional vectors and data matrix $D \in \mathbf{R}^{p \times n}$ is generated. Let us assume that each observed image is a linear combination of r factor images, aggregated in matrix $A \in \mathbf{R}^{p \times r}$. Typically, $r < n \ll p$ is expected. Every factor image has its time-activity curve, $x_j = [x_{1,j}, \dots, x_{n,j}]'$; therefore, time-activity matrix $X \in \mathbf{R}^{n \times r}$ is created. The only that we have is data-storage matrix D, and we would like to estimate factor image matrix A and factor curve matrix X.

The model of the factor analysis can be written in matrix form as

$$D = AX' + E, \tag{1}$$

where $E \in \mathbf{R}^{p\times n}$ is noise matrix with i.i.d. elements with variance ω^{-1}. Matrix D aggregates measurements of radioactive particles with Poisson distributions which can be approximated by Gauss normal distribution; therefore, covariance matrix of noise matrix E can be found using correspondence analysis [3] as

$$f(D|A, X, \omega) = \mathrm{tN}_D(AX', \omega^{-1}\Omega_p \otimes \Omega_n), \tag{2}$$
$$\Omega_p = \mathrm{diag}(D\mathbf{1}_{n,1}), \Omega_n = \mathrm{diag}(\mathbf{1}_{1,p}D), \tag{3}$$

where tN(.) denotes truncated normal distribution, diag(.) denotes square diagonal matrix with diagonal vector as an argument, $\mathbf{1}_{k,l}$ denotes matrix of ones of subscripted dimensions, and $\otimes$ denotes Kronecker matrix product.

A prior model of parameters follows as:

$$f(\omega) = G_\omega(\vartheta_0, \rho_0), \tag{4}$$
$$f(X|\Upsilon) = \mathrm{tN}_X(0_{n,r}, \Omega_n \otimes \Upsilon^{-1}), \tag{5}$$
$$\Upsilon = \mathrm{diag}(v), v = [v_1, \ldots, v_r]', \tag{6}$$
$$f(v) = \prod_{j=1}^{r} G_{v_j}(\alpha_{j,0}, \beta_{j,0}), \tag{7}$$
$$f(A) = \mathrm{tN}_A(0_{p,r}, \Omega_p \otimes I_r), \tag{8}$$

where $\vartheta_0, \rho_0 \in \mathbf{R}$ are scalar prior parameters, v is vector of hyper-parameters with prior parameters $\alpha_0, \beta_0 \in \mathbf{R}$, G(.) is gamma distribution, and I_r is identity matrix of dimensions $r \times r$.

The difference between principal component analysis (PCA) and factor analysis is truncation in equations (5) and (8); in addition, for non-truncated distributions in (5) and (8), variational solution converges to the PCA solution [8].

With respect to Variational Bayes method [8], a logarithm of joint distribution $f(D, A, X, \Upsilon, \omega|r)$ is computed and the resulting approximate posterior marginals are recognized in form:

$$\tilde{f}(\omega|D, r) = G_\omega(\vartheta, \rho), \qquad \tilde{f}(X|D, r) = \mathrm{tN}_X(\mu_X, \Sigma_X \otimes \Upsilon), \tag{9}$$
$$\tilde{f}(v|D, r) = \prod_{j=1}^{r} G_{v_i}(\alpha_i, \beta_i), \qquad \tilde{f}(A|D, r) = \mathrm{tN}_A(\mu_A, \Omega_p^{-1} \otimes \Sigma_A), \tag{10}$$

and the associated shaping parameters are

$$\mu_A = \hat{\omega}\Omega_p D\Omega_n \widehat{X}\Sigma_A, \qquad \Sigma_A = \left(\hat{\omega}\widehat{X'\Omega_n X} + I_r\right)^{-1},$$
$$\mu_X = \hat{\omega}\Omega_n D'\Omega_p \widehat{A}\Sigma_X, \qquad \Sigma_X = \left(\hat{\omega}\widehat{A'\Omega_p A} + \widehat{\Upsilon}\right)^{-1},$$

$$\alpha = \alpha_0 + \frac{n}{2}\mathbf{1}_{r,1}, \qquad \beta = \beta_0 + \frac{1}{2}\operatorname{diag}\left(\widehat{X'\Omega_n X}\right),$$
$$\vartheta = \vartheta_0 + \frac{np}{2}, \qquad \rho = \rho_0 + \frac{1}{2}\operatorname{tr}\left(DD' - \widehat{A}\widehat{X}'D' - D\widehat{X}\widehat{A}'\right) + \frac{1}{2}\operatorname{tr}\left(\widehat{A'A}\widehat{X'X}\right).$$

The necessary moments of previous distributions are $\widehat{\Upsilon} = \operatorname{diag}(\alpha \circ \beta^{-1})$, where $\circ$ denotes Hadamard product, $\widehat{\omega} = \frac{\vartheta}{\rho}$ and moments of truncated normal distribution are computed with respect to Appendix A.

3 Factor Analysis with a Prior Mask on Factor Images (FAM)

In the previous section, we revised classical factor analysis without any additional assumptions. Our long-way intention is to automatically analyse a scintigraphical sequence, not only set out factor images and factor curves. This section models a prior probabilistic mask on factor images, i.e. matrix A. This is motivated by unsatisfactory separation of tissue background from other organs, parenchyma and pelvis at most, in the previous methods.

3.1 Modeling of Factor Images

Our new model should better separate tissue background and the proper organ; consequently, the relation factor curve will be better too. In addition, a probability mask of location of a factor will be obtained.

Consider prior probability mask of A of the same size as A, $\mathbf{i} \in \mathbf{R}^{p\times r}$, where

$$\mathbf{i}_{i,j} = \begin{cases} 1 & i\text{th pixel belongs to the } j\text{th factor} \\ 0 & i\text{th pixel not belongs to the } j\text{th factor} \end{cases}, \text{ with prior}$$

$$f(\mathbf{i}_{i,j}) = \operatorname{Exp}(\lambda_{ij,0}). \tag{11}$$

In places with pixels which not belong to the related factor, the noise with normal distribution with zero mean value is expected. For the jth factor, these pixels have distribution $N(0, \xi_{0,j}^{-1})$. Here, $\xi_{0,j}$ is covariance of these zero-mean-pixels of the jth factor hyperparametrized by ϕ and ψ as gamma distribution; for $\xi_0 = [\xi_{0,1}, \ldots, \xi_{0,r}]', \Xi_0 = \operatorname{diag}(\xi_0)$ is

$$f(\xi_0) = \prod_{j=1}^{r} G_{\xi_{0,j}}(\phi_{j,0}, \psi_{j,0}). \tag{12}$$

In case of non-zero-value-pixels of the jth factor, uniform distribution is expected in the form $U(0, A_j^{\max})$ for $A_j^{\max} = \max_i A_{i,j}$. In general, the second parameter of uniform distribution can be replaced by Pareto distribution or Gamma distribution, but the maximum of the jth column of matrix A is almost the same.

Generally, matrix A is modeled as independent elements as

$$f(A) = \prod_{i=1}^{p}\prod_{j=1}^{r} f(a_{i,j}), \tag{13}$$

and each element is modeled as

$$f(a_{i,j}) = U(0, A_j^{\max})^{\mathbf{i}_{i,j}}\, \mathrm{tN}_{a_{i,j}}(0, \xi_{0,j}^{-1})^{(1-\mathbf{i}_{i,j})}, \tag{14}$$

where exponentation of $\mathbf{i}_{i,j}$ or $(1-\mathbf{i}_{i,j})$ provides an affilation to the informative or non-informative part of the factor image.

3.2 Variational Solution

The joint likelihood for the new model, $f(D, A, X, \Upsilon, \Xi_0, \mathbf{i}, \omega | r)$, is obtained by replacing (8) in model (2) - (8) with prior information (11), (12), and (14). Using Variational Bayes method, the following posterior densities are identified:

$$\begin{aligned}
\tilde{f}(X|D,r) &= N(\mu_X, I_n \otimes \Sigma_X), & \tilde{f}(v|D,r) &= \prod_{j=1}^{r} G_{v_j}(\alpha_j, \beta_j),\\
\tilde{f}(\omega|D,r) &= G_\omega(\vartheta, \rho), & \tilde{f}(a_i|D,r) &= N_{a_i}(\mu_{a_i}, \Sigma_{a_i}),\\
\tilde{f}(\xi_0|D,r) &= G_{\xi_0}(\phi, \psi), & \tilde{f}(\mathbf{i}_{i,j}|D,r) &= \mathrm{Exp}_{\mathbf{i}_{i,j}}(\lambda_{i,j}),
\end{aligned}$$

with shaping parameters

$$\begin{aligned}
\Sigma_X &= \left(\widehat{\omega}\widehat{A'A} + \widehat{\Upsilon}\right)^{-1}, & \mu_X &= \widehat{\omega} D' \widehat{A} \Sigma_X,\\
\alpha &= \alpha_0 + \frac{n}{2}\mathbf{1}_{r,1}, & \beta &= \beta_0 + \frac{1}{2}\,\mathrm{diag}(\widehat{X'X}),\\
\vartheta &= \vartheta_0 + \frac{pn}{2}, & \rho &= \rho_0 + \frac{1}{2}\,\mathrm{tr}\left(DD' - \widehat{A}\widehat{X}'D' - D\widehat{X}\widehat{A}'\right) +\\
& & &\quad + \frac{1}{2}\,\mathrm{tr}\left(\widehat{A'A}\widehat{X'X}\right),\\
\Sigma_{a_i} &= \left(\widehat{\omega}\sum_{k=1}^{n}(\widehat{x_k' x_k}) + \widehat{\Xi_0}(I_r - \widehat{\iota_i})\right)^{-1}, & \mu_{a_i} &= \left(\Sigma_{a_i}\left(\widehat{\omega}\sum_{k=1}^{n}(\widehat{x}_k d_{i,k})'\right)\right)',\\
\phi_j &= \left(\phi_{j,0} + \frac{1}{2}\sum_{i=1}^{p}(1 - \widehat{\mathbf{i}_{i,j}})\right), & \psi_j &= \left(\psi_{j,0} + \frac{1}{2}\sum_{i=1}^{p}(1 - \widehat{\mathbf{i}_{i,j}})\widehat{a_{i,j}^2}\right),\\
\lambda_{i,j} &= \lambda_{ij,0} - \ln A_j^{\max} - \frac{1}{2}\ln\widehat{\xi_0} + \frac{1}{2}\widehat{a_{i,j}\xi_0 a_{i,j}}, & &
\end{aligned}$$

where $\iota_i = \mathrm{diag}(\mathbf{i}_{i,:})$.

The required moments are $\widehat{\Upsilon} = \mathrm{diag}(\alpha \circ \beta^{-1})$, $\widehat{\Xi_0} = \mathrm{diag}(\phi \circ \psi^{-1})$, $\widehat{\omega} = \frac{\vartheta}{\rho}$, $\widehat{\mathbf{i}_{i,j}} = \frac{1}{\lambda_{i,j}}$, and moments of truncated normal distribution are computed with respect to Appendix A.

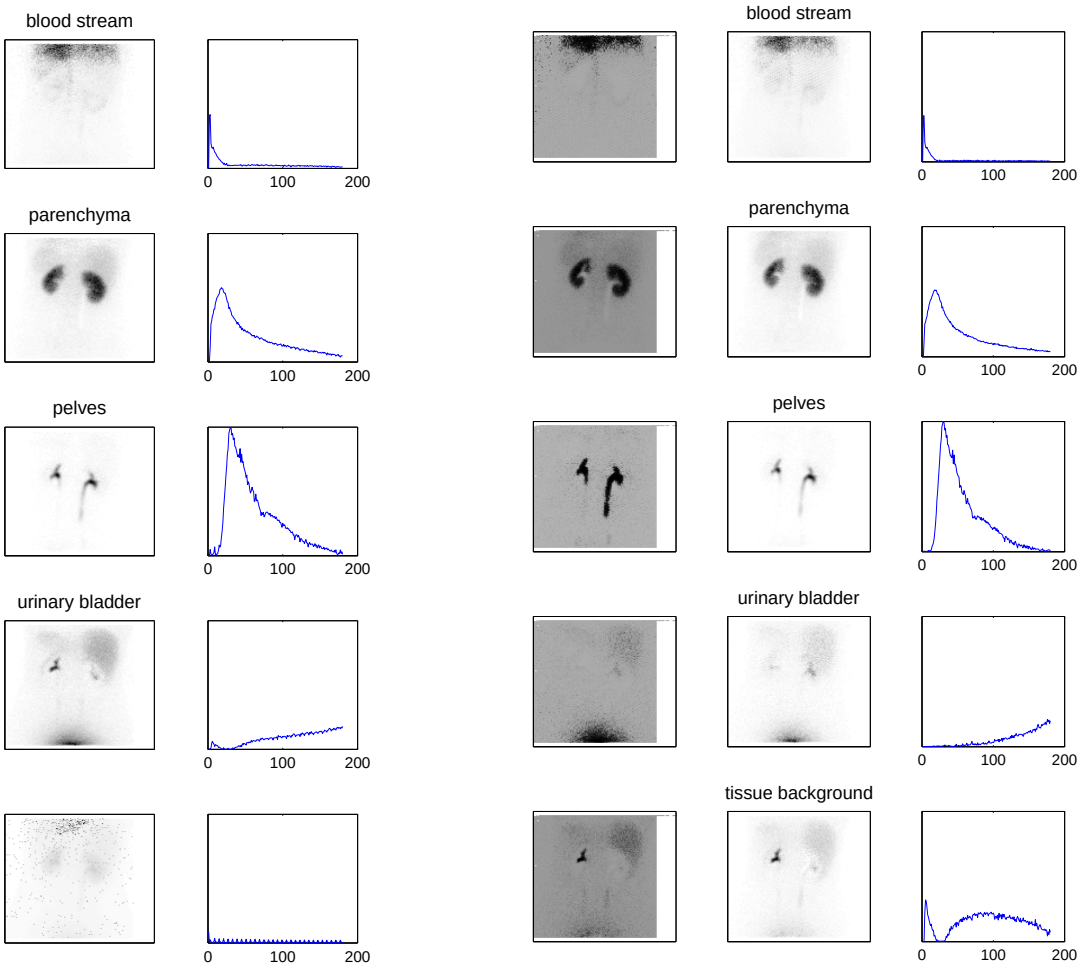

Figure 1: The results from the FA algorithm (left) and from the FAM algorithm (right)

4 Feasibility Study with Clinical Data

The previous algorithms were tested on a scintigraphic study. Factor images and factor curves were estimated in the case of FA and FAM algorithms; next, the resulting estimates and computed convolution kernels of parenchyma are studied.

4.1 Estimation of Factor Images and Curves

The first task is an estimation and separation of factors. Figure 1 shows the results from the FA algorithm, section 2, and from the FAM algorithm, section 3. From the left, FA estimates factor images, i.e. $\widehat{A}$, and factor curves, i.e. $\widehat{X}$; FAM estimates probability mask of factor images, i.e. $\widehat{\mathbf{i}}$, factor images, i.e. $\widehat{A}$, and factor curves, i.e. $\widehat{X}$. Both algorithms automatically estimated as the strongest factors blood background, renal parenchyma,

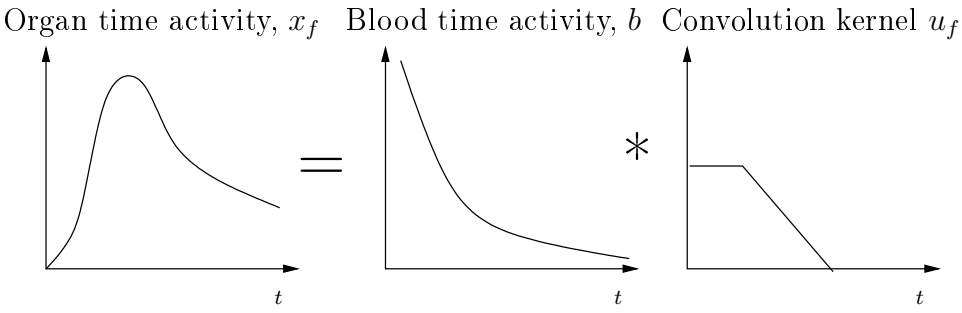

Figure 2: Theoretical decomposition of a factor curve

renal pelves, and urinary bladder; in addition, FAM estimated tissue background as the last significant factor.

The main differences between FA and FAM are in the beginning of the factor curves, especially of renal pelves and urinary bladder. In biological restriction, pelves curve should be at a zero level for the first $2-3$ minutes, i.e. $12-18$ frames. This restriction is well satisfied by FAM in contrast with FA with significant activity at the beginning of the curve. The same can be seen by urinary bladder; here, non-zero beginning is caused by improper separation of tissue background and bladder by FA algorithm. This zero-level-plateaus are very important from the biological view. In addition, this fact implies that the factor images of pelves and urinary bladder are undoubtedly better separated from tissue background by FAM then by FA.

4.2 Estimation of Convolution Kernel of Parenchyma

In the biological point of view, each time activity curve of factor is a convolution between blood and its specific convolution kernel [6, 2, 9]. Moreover, this convolution kernel is positive and its shape is shown in Figure 2. There should be a constant positive plateau and then linear or exponential decline to zero. From the length the plateau can be identified an important diagnostic coefficient - the transit time.

Figure 3 shows convolution kernels of parenchyma computed using Fourier transform. The result of FA is in the top, the result of FAM is the bottom row. In FA case, the peak at the beginning of the convolution kernel implies that separation of parenchyma and tissue background are not perfect [2]. From this point of view, FAM gives more appropriate results.

5 Discussion

The results presented in Section 4 suggest that factor analysis with integrated probability mask on factor images has a potential to improve the whole estimative procedure. However, more improvement is necessary for automatic estimation of diagnostic coefficients, which can be compared with experts. For example, the information from probabilistic mask $\widehat{\mathbf{i}}$ can be adopted for automatic selection of position of the single organs and consecutive computations. Study and usage of this fact is suggestion for future work.

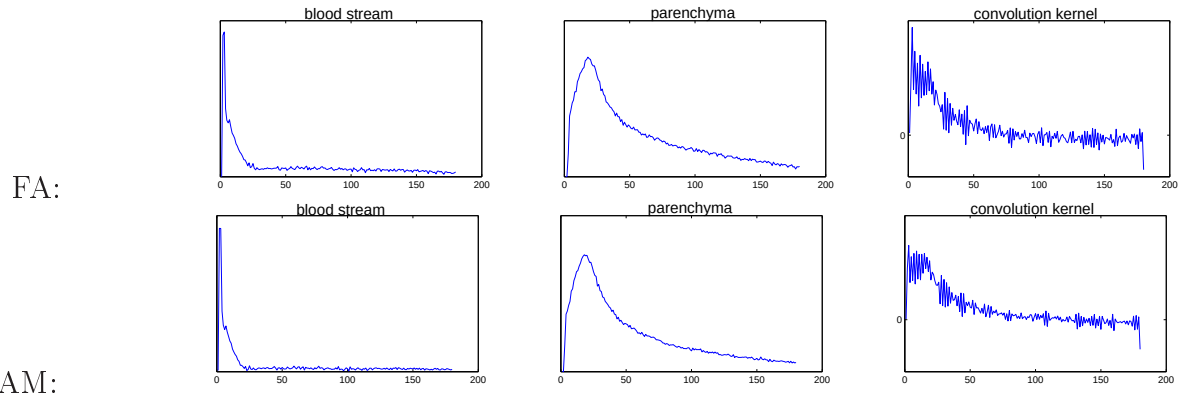

Figure 3: Convolution kernel of parenchyma (right) obtained from blood curve (left) and parenchyma curve (center).

Modeling of non-zero pixels as uniform distribution (14) is motivated by observation and seems to be better than modeling as normal distribution. However, more appropriate distribution or method should be used for modeling of histogram of the matrix A. It could lead to better separation of the factors.

With respect to study of non-zero priors of factor images, factor curves can be studied in the same way. A prior zero mean value of X is chosen due to computable reasons; nevertheless, more appropriate mean value can be computed [9].

6 Conclusion

A new model of factor images in functional analysis of scintigraphic dynamic sequences is proposed. The main addition is the dividing of pixels of factor images into informative and non-informative parts. The resulting algorithm is obtained using Variational Bayes method based on modeling parameters as independent components. Feasibility of solution is shown on clinical data from renal scintigraphy and compared with classical factor analysis where is demonstrated an improvements over previous methods. An automatic estimation of important diagnostic parameters will follow so as an extensive clinical study.

Appendix

A Moments of truncated Normal Distribution

Scalar truncated normal distribution

$$tN_x(x|\mu, r) = \alpha\sqrt{2}\exp\left(-\frac{(x-\mu)^2}{2r}\right), \; x > 0, \tag{15}$$

has moments

$$\widehat{x} = \mu + r\alpha\sqrt{2}\exp\left(-\frac{\mu^2}{2r}\right), \quad \widehat{x^2} = r + \mu\widehat{x},$$

where $\alpha^{-1} = \sqrt{\pi r}(1 - \mathrm{erf}(-\frac{\mu}{\sqrt{2r}})$ and erf is the error function.

References

[1] I. Buvat, H. Benali, and R. Di Paola. *Statistical distribution of factors and factor images in factor analysis of medical image sequences.* Physics in Medicine and Biology **43** (1998), 1695–1711.

[2] E. Durand, M. Blaufox, K. Britton, O. Carlsen, P. Cosgriff, E. Fine, J. Fleming, C. Nimmon, A. Piepsz, A. Prigent, et al. International Scientific Committee of Radionuclides in Nephrourology (ISCORN) consensus on renal transit time measurements. In 'Seminars in nuclear medicine', volume 38, 82–102. Elsevier, (2008).

[3] J. Fine and A. Pouse. *Asymptotic study of the multivariate functional model. application to the metric of choise in principal component analysis.* Statistics **23** (1992), 63–83.

[4] J. Fleming and P. Kemp. *A comparison of deconvolution and the Patlak-Rutland plot in renography analysis.* Journal of Nuclear Medicine **40** (1999), 1503.

[5] R. Klein, R. Beanlands, A. Adler, and R. deKemp. Model-based factor analysis of dynamic sequences of cardiac positron emission tomography. In 'Nuclear Science Symposium Conference Record, 2008. NSS'08. IEEE', 5198–5202. IEEE, (2009).

[6] A. Kuruc, W. Caldicott, and S. Treves. *An improved deconvolution technique for the calculation of renal retention functions.* Computers and Biomedical Research **15** (1982), 46–56.

[7] G. Lueck, T. Kim, P. Burns, and A. Martel. *Hepatic perfusion imaging using factor analysis of contrast enhanced ultrasound.* Medical Imaging, IEEE Transactions on **27** (2008), 1449–1457.

[8] V. Šmídl and A. Quinn. *The Variational Bayes Method in Signal Processing.* Springer, (2005).

[9] O. Tichý. Integral models for dynamic renal scintigraphy, (2010). Thesis, FNSPE CTU.

[10] M. Šámal, M. Kárný, H. Sůrová, E. Maříková, and Z. Dienstbier. *Rotation to simple structure in factor analysis of dynamic radionuclide studies.* Physics in Medicine and Biology **32** (1987), 371–382.

[11] M. Šámal, M. Kárný, H. Sůrová, P. Pěnička, E. Maříková, and Z. Dienstbier. *On existence of unambiguous solution in factor analysis of dynamic studies.* Physics in Medicine and Biology **34** (1989), 223–228.